INTERNATIONAL JOURNAL FOR NUMERICAL METHODS IN FLUIDS
Int. J. Numer. Meth. Fluids 2005; **47**:995–1001
Published online 24 January 2005 in Wiley InterScience (www.interscience.wiley.com). DOI: 10.1002/fld.865

An adaptive mesh adjoint data assimilation method applied to free surface flows

F. Fang*,†, C. C. Pain, M. D. Piggott‡, G. J. Gorman and A. J. H. Goddard

Applied Modelling and Computation Group, Department of Earth Science and Engineering, Imperial College, Prince Consort Road, London, SW7 2BP, U.K.

SUMMARY

In this paper, we describe the construction of a three-dimensional adaptive mesh data assimilation method for oceanographic/coastal applications, including a free surface. This is the first attempt at introducing a moving computational domain into an adjoint model with mesh adaptivity. We also provide insight into the feasibility and reliability of the adaptive mesh adjoint model. The use of differing adapting meshes for forward and adjoint problems is considered here, where each mesh is optimized with respect to the individual properties of each solution. The free surface test case considered is that of flow in a two-dimensional vertical fluid slice. In this test case the sea surface elevation boundary conditions is optimized by assimilating sea surface height observations. The feasibility of an assimilation approach on adapting moving domains is demonstrated by comparison with a fixed mesh result.

KEY WORDS: data assimilation; free surface; adjoint; finite element; unstructured adaptive mesh

1. INTRODUCTION

With the rapid development of observational measurement techniques, such as in situ measurements and remote sensing, there is an increasing interest in the assimilation of advanced observations into models. The assimilation of observations may be used to optimize unknown model inputs such as initial and boundary conditions, sea surface elevation, bottom friction coefficients, and wind stress, see for example References [1, 2]. The adjoint method is a technique which can efficiently assimilate observed data into simulations [3, 4]. It is also an effective tool for performing sensitivity analysis, which has applications in observation planning as well as model development [4, 5]. The investigation of the adjoint method has been

*Correspondence to: F. Fang, Applied Modelling and Computation Group, Department of Earth Science and Engineering, Imperial College, Prince Consort Road, London, SW7 2BP, U.K.
†E-mail: f.fang@imperial.ac.uk, URL: http://amcg.ese.imperial.ac.uk
‡E-mail: m.d.piggott@imperial.ac.uk

Contract/grant sponsor: EPSRC; contract/grant number: GR/60898

Received 27 April 2004
Revised 5 October 2004
Accepted 6 October 2004

applied to 4D variational data assimilation [6–8]. The adjoint approach has also been extended to include a free surface (see for example References [9, 10] in the case of depth averaged shallow water models), and used to increase the accuracy of hydrodynamic models by assimilating available data to improve velocity boundary conditions. Our long-term aim is to develop a robust and effective adjoint model to assimilate available data in space and time into a spatially 3D prognostic model with a free surface. To do this we introduce a new adaptive mesh adjoint model, which has the following features:

- Use of a non-hydrostatic Navier–Stokes finite element solver on 3D anisotropic unstructured meshes [11, 12];
- introduction of mesh adaptivity into the adjoint model [13];
- incorporation of a free surface (moving computational domain [14]) into the adjoint model;
- automatic production of a hierarchy of increasingly fine meshes to accelerate inversion.

In the following section, the formulation of the adjoint model for data assimilation with a free surface is given. This is followed by a discussion of the related numerical techniques and the special treatment of the free surface. Finally, a simple test case is presented of 2D channel flow, where the adjoint model is applied to invert for free surface elevation at an inlet boundary.

2. ADJOINT MODEL FORMULATION FOR DATA ASSIMILATION WITH A FREE SURFACE

2.1. The objective functional

The objective of the optimization, which is achieved by adjusting the uncertainties (control variables) in the model, is to minimize an objective functional. In this investigation the objective functional is designed for inverting sea surface elevation at the inlet of a flow channel, and measures the misfit between the numerical solution and observed data:

$$\mathscr{J}(\zeta,\zeta_{\mathrm{b}}) \equiv \frac{1}{2}\int_t\int_\Omega \sum_{k=1}^{N} (\zeta-\zeta_{\mathrm{o},k})^{\mathrm{T}} W_k (\zeta-\zeta_{\mathrm{o},k})\,\mathrm{d}\Omega\,\mathrm{d}t + \frac{1}{2}\int_t\int_{\partial\Omega} \lambda(\zeta_{\mathrm{b}}-H)^{\mathrm{T}}(\zeta_{\mathrm{b}}-H)\,\mathrm{d}(\partial\Omega)\,\mathrm{d}t \tag{1}$$

Here, k represents an index of detectors which yield observations, with N being the total number of such detectors; ζ_{b} represents the unknown water elevation at the boundary, defined here as a *control variable* to be optimized for using the adjoint method; $\zeta \equiv \zeta(x,y,t)$ is the free surface elevation; $\zeta_{\mathrm{o},k}$ is the observed free surface elevation at detector k; H is the average water depth; W_k is a scalar weight associated with the misfit between the numerical solution and observation at detector k; λ is a suitable scalar weighting for the penalty term in (1) which is used to avoid spurious functional minima [4]; Ω is the computational domain and $\partial\Omega$ is its boundary. A non-linear conjugate gradient method is used to minimize this functional [15].

2.2. The forward model

The numerical model used in this investigation employs 3D P_1P_1 (piecewise-linear representation of both velocity and pressure) tetrahedral finite elements with theta time stepping. Due to the well-known spurious modes present with this element choice [16] a fourth-order pressure filter is employed to aid stability. In addition, standard Petrov–Galerkin weightings [17] are used to improve numerical stability in the presence of advection dominated flows. The assumption of hydrostatic balance is not invoked here. For additional numerical details see References [11, 18]. The underlying model equations are thus comprised of the Navier–Stokes momentum and continuity equations

$$\frac{\partial \boldsymbol{u}}{\partial t} + \boldsymbol{u}\cdot\nabla\boldsymbol{u} + f\boldsymbol{k}\times\boldsymbol{u} = -\frac{1}{\rho}\nabla p - s\boldsymbol{k} + \mathbf{D}, \quad \nabla\cdot\boldsymbol{u} = 0 \tag{2}$$

and the kinematic free surface equation for the free surface elevation ζ, measured from some fixed datum,

$$\frac{\partial \zeta}{\partial t} + u\frac{\partial \zeta}{\partial x} + v\frac{\partial \zeta}{\partial y} = w \tag{3}$$

where $\boldsymbol{u} \equiv (u, v, w)^{\mathrm{T}}$ is the velocity, p is the pressure, $\mathbf{D}$ contains the viscous terms expressed in stress form, f represents the Coriolis inertial force, ρ is the density, s represents the buoyancy force, and $\boldsymbol{k} = (0, 0, 1)^{\mathrm{T}}$. For simplicity, here density is assumed constant and thus the pressure p consists of hydrostatic $p_h(z)$ and non-hydrostatic $p_{nh}(x, y, z, t)$ components. The hydrostatic component of pressure balances exactly the constant buoyancy force and both terms are, therefore, dropped at this stage. Taking into account the free surface, pressure may be written $p = p_{nh} + \rho g\zeta$, and (2) then takes the form

$$\frac{\partial \boldsymbol{u}}{\partial t} + \boldsymbol{u}\cdot\nabla\boldsymbol{u} + f\boldsymbol{k}\times\boldsymbol{u} + g\left(\frac{\partial \zeta}{\partial x}, \frac{\partial \zeta}{\partial y}, 0\right)^{\mathrm{T}} + \frac{1}{\rho}\nabla p_{nh} - \mathbf{D} = 0, \quad \nabla\cdot\boldsymbol{u} = 0 \tag{4}$$

2.3. Formulation of an adjoint model

There are two ways to derive the adjoint model. One is to obtain the discrete adjoint model directly from the discrete forward model, consistency with the discrete forward model is then guaranteed. Alternatively, the adjoint model may be derived from the continuous forward model equations. Since the forward and adjoint model equations are similar, it is relatively straightforward to construct a resulting adjoint numerical code from a forward code. The derivation of the adjoint equations can be done using the Euler–Lagrange method. This is achieved by multiplying the tangent linear model by dual variables $u^*, v^*, w^*, p^*, \zeta^*$, and applying Green's theorem (in space and time), to obtain the following adjoint model:

$$\begin{aligned} &-\frac{\partial \boldsymbol{u}^*}{\partial t} - \boldsymbol{u}\cdot\nabla\boldsymbol{u}^* - f\boldsymbol{k}\times\boldsymbol{u}^* - \frac{1}{\rho}\nabla p_{nh}^* - \mathbf{D}^* \\ &-(\nabla\boldsymbol{u}^*)^{\mathrm{T}}\boldsymbol{u} - \left(\zeta\frac{\partial \zeta^*}{\partial x}, \zeta\frac{\partial \zeta^*}{\partial y}, \zeta^*\right)^{\mathrm{T}}\delta(z-\zeta) = (S_u, S_v, S_w)^{\mathrm{T}} \end{aligned} \tag{5}$$

$$\nabla \cdot (-\rho^{-1}\boldsymbol{u}^*) = S_p \tag{6}$$

$$-\frac{\partial \zeta^*}{\partial t} - \frac{\partial u\zeta^*}{\partial x} - \frac{\partial v\zeta^*}{\partial y} - g\frac{\partial u^*}{\partial x} - g\frac{\partial v^*}{\partial y} = S_\zeta \tag{7}$$

Here, $S_u, S_v, S_w, S_p, S_\zeta$ are the source terms at the detectors where the observations are available, i.e. the misfit of the numerical solution u, v, w, p, ζ and the corresponding observations respectively: $S_u = \sum_{k=1}^{N} (u - u_{\mathrm{o},k})\delta(x - x_{\mathrm{o},k})\delta(y - y_{\mathrm{o},k})\delta(z - z_{\mathrm{o},k})$, with the other terms being defined analogously, here $\delta(\cdot)$ is the Dirac-delta function, $(x_{\mathrm{o},k}, y_{\mathrm{o},k}, z_{\mathrm{o},k})$ is the location of detector k, and $(u_{\mathrm{o},k}, v_{\mathrm{o},k}, w_{\mathrm{o},k})$ is the observed velocity. In addition, these source terms are 'spread' over the discrete numerical mesh via convolution with a Gaussian kernel. The adjoint solution variables are used to calculate the gradient (see for example References [19, 20]) of the objective functional (1) for use in the nonlinear conjugate gradient minimization.

3. MESH ADAPTIVITY AND THE FREE SURFACE

The meshes for the forward and adjoint components of the simulation are dynamically adapted to best capture the distinct solution characteristics of each. In this work, a simple *a priori* interpolation theory based error measure is employed; the curvature of the solution fields are thus used to guide mesh refinements via local optimization [12]. In addition, the forward model possesses a free surface which results in a moving domain, this additional complexity is handled here using a mesh which is allowed to 'move' in the vertical, with nodes at the free surface staying on the free surface and nodes at the sea bed remaining fixed. A combination of mesh optimization, which primarily comprises local topological operations on the mesh structure, and mesh movement is thus employed [14]. The adjoint equations are solved in the same domain as the forward model, i.e. the domain controlled by the forward model's free surface, and are also based on the forward solution fields. Therefore, to run the adjoint model all information from the forward model from each time level is stored, i.e. the solution fields and the forward mesh. The procedure for running the adjoint model is thus to: (i) obtain the computational domain from the forward water elevation solution at the current time level; (ii) transform the adjoint mesh from the adjoint domain at the previous time level into the current computation domain via vertical mesh movement; (iii) interpolate the forward solutions from the forward mesh onto the resulting adjoint mesh.

4. TEST CASE AND DISCUSSION

The adjoint model is now applied to invert for the boundary condition (free surface height ζ_b) at the inlet in a 2D channel flow problem (Figures 1 and 2). The length of the channel is 100 m. The average water depth is $H = 5.0$ m. The free surface height at the inlet is inverted by assimilating a pseudo-observation, in this case the free surface elevation. This is obtained at the middle of the channel ($x = 50$ m), via an identical twin experiment, by running the forward model with the specified control variable ζ_{exac} (free surface height at the inlet, $\zeta_{\mathrm{exac}} = H + 0.3\sin(2\pi t/45)$ and the initial conditions: $\zeta_0 = 5.0$ m and $u_0 = 0.3\ \mathrm{ms}^{-1}$. Given the inverted free surface height at the boundary, ζ_b, the corresponding inflow velocity u_b can be calculated by assuming: $u_\mathrm{b} = U_0 + (\zeta_\mathrm{b} - H)\sqrt{g/\zeta_\mathrm{b}}$, for a background inflow

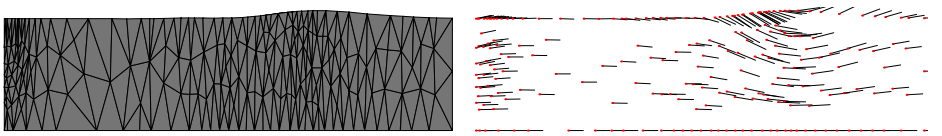

Figure 1. Adapted mesh for the forward problem (left) and flow velocity vectors (right). The maximum velocity is approximately $0.5\,\mathrm{ms}^{-1}$. Figures have been stretched by a factor of 5 in the vertical.

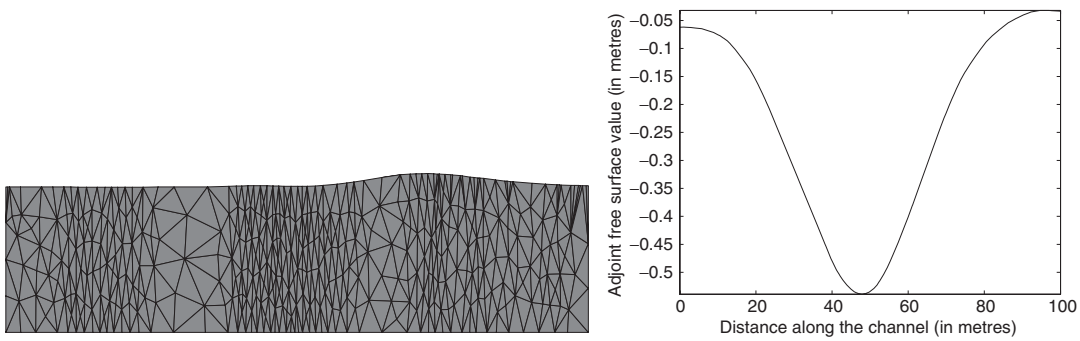

Figure 2. Adapted mesh for the adjoint problem (left) and the adjoint free surface profile along the channel (right). The mesh is finer where the curvature of the adjoint free surface variable is large.

velocity of $U_0 = 0.3\,\mathrm{ms}^{-1}$ (see also [10]). Stress free boundary conditions are applied at the outlet. With an initial guess of $\zeta_\mathrm{b} = 5.0\,\mathrm{m}$ and the corresponding $u_\mathrm{b} = 0.3\,\mathrm{ms}^{-1}$ at the inlet, the whole inversion starts from the background flow and average water depth. The meshes for the forward and adjoint models are adapted from their original regular meshes with a mesh size of 0.5 m in the horizontal and 1.0 m in the vertical. Bounds on the minimum and maximum adapted mesh element sizes are set to be 0.3 and 8.0 m in the horizontal, and 0.5 and 1.0 m in the vertical, respectively. Figure 1 shows: (a) an example of the forward mesh, and (b) the corresponding flow vector structure for the forward model at $t = 34\,\mathrm{s}$ from the forward solution with the optimized boundary condition. Figure 2 shows: (a) the adaptive mesh for the adjoint model at the same time level as shown in Figure 1 ($t = 34\,\mathrm{s}$), and (b) the corresponding profile of the adjoint free surface elevation. The advantage of the different adaptive meshes for the forward and adjoint model is that the meshes are adapted to best suit their own flow features. The adjoint mesh is finer near the observation location ($x = 50\,\mathrm{m}$), which is adapted according to the curvature of the adjoint free surface elevation (see Figure 2). For the forward model at the beginning of the simulation time a finer mesh is formed at the inlet, with a much coarser mesh towards the outlet (where all solution fields are linear and hence well approximated using fewer elements). This region of enhanced mesh resolution then spreads along the flow direction as the surface waves propagate. Figure 3 shows a plot of both the exact free surface height and the optimized inlet boundary condition ζ_b in the case of adapting forward and adjoint meshes, as well as fixed uniform meshes (comprising 300 cells in the horizontal and 5 levels in the vertical) for comparison purposes. Note that the fixed mesh has 1806 nodes, whereas the adaptive simulation has 225 and 435 nodes for

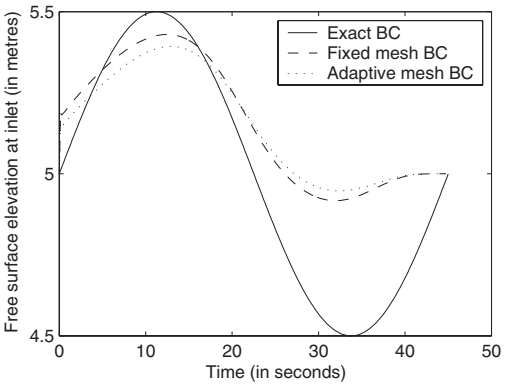

Figure 3. Boundary condition at the inlet $x = 0$ for the exact forward run, and inverted results for both fixed and adapting meshes for the forward and adjoint problems.

the forward and adjoint meshes shown in Figures 1 and 2, respectively, and takes less than half the computational time. The sinusoidal nature, amplitude and period of the free surface field are well captured during the first half period. However, the inlet boundary condition cannot be optimized during the second half period. The reason for this is that there is no sensitivity information during the second half of the simulation period (22.5–45 s). It takes approximately 22.5 s for the information to propagate from the detector ($x = 50\,\mathrm{m}$) to the inlet (in this test case, the phase celerity is $c = \sqrt{gH} = 2.2\,\mathrm{ms}^{-1}$ for shallow water as here gravity is $g = 1.0\,\mathrm{ms}^{-2}$).

5. CONCLUDING REMARKS

In this paper we have reported a first attempt at the application of mesh adaptivity to an adjoint model for data assimilation with a free surface. The inclusion of 3D flow dynamics with mesh adaptivity and a free surface (moving domain) poses new challenges to the implementation of adjoint models. Future work will benefit from this novel contribution, e.g. the use of a hierarchy of finer meshes, naturally available via the adaptivity approach, to accelerate the inversion procedure. The adjoint and forward models can have their own flexible computation meshes, which allows the adapted meshes to conform to the forward and adjoint solution features independently. A simple example of the application of this adjoint model has been given as a means to demonstrate the feasibility of performing data assimilation with mesh adaptivity and numerical techniques for free surface movement. Preliminary results have been presented which demonstrate the ability to invert for free surface elevation at an open boundary by assimilating observations. Further developments, for example to the case of non-constant density stratification, are ongoing, as are applications to different oceanic cases.

ACKNOWLEDGEMENTS

We would like to thank Prof. I. M. Navon and Drs G. M. Copeland and I. Gejadze for many helpful discussions. This work was carried out under funding from the EPSRC grant GR/60898.

REFERENCES

1. Bennett AF. *Inverse Methods in Physical Oceanography*. Cambridge University Press: Cambridge, 1992.
2. Tziperman E, Thacker WC, Long RB, Hwang SM, Rintoul S. Oceanic data analysis using a general circulation model. Part II: a North Atlantic model. *Journal of Physical Oceanography* 1992; **22**:1458–1485.
3. Talagrand O, Courtier P. Variational assimilation of meteorological observations with the adjoint vorticity equation (I). Theory. *Quarterly Journal of the Royal Meteorological Society* 1987; **113**:1311–1328.
4. Gunzburger MD. *Perspectives in Flow Control and Optimization*. SIAM: Philadelphia, 2003.
5. Farrell BF, Moore AM. An adjoint method for obtaining the most rapidly growing perturbation to oceanic flows. *Journal of Physical Oceanography* 1992; **22**(4):338–349.
6. Wenzel M, Schröter J, Olbers D. The annual cycle of the global ocean circulation as determined by 4D VAR data assimilation. *Progress in Oceanography* 2001; **48**(1):73–119.
7. Daescu DN, Navon IM. Adaptive observations in the context of 4D-Var data assimilation. *Meteorology and Atmospheric Physics* 2004; **85**(4):205–226.
8. Courtier P. A strategy for operational implementation of 4D-Var, using an incremental approach. *Quarterly Journal of the Royal Meteorological Society* 1994; **120**:1367–1387.
9. Bosseur F, Flori F, Orenga P. Identification of boundary conditions in a nonlinear shallow water flow. *Computers and Mathematics with Applications* 2002; **43**:1559–1573.
10. Annan JD. Hindcasting coastal sea levels in Morecambe Bay. *Estuarine, Coastal and Shelf Science* 2001; **53**:459–466.
11. Ford R, Pain CC, Piggott MD, Goddard AJH, de Oliveira CRE, Umpleby AP. A nonhydrostatic finite-element model for three-dimensional stratified oceanic flows. Part I: Model formulation. *Monthly Weather Review* 2004; **132**(12):2816–2831.
12. Pain CC, Umpleby AP, de Oliveira CRE, Goddard AJH. Tetrahedral mesh optimisation and adaptivity for steady-state and transient finite element calculations. *Computer Methods in Applied Mechanics and Engineering* 2001; **190**:3771–3796.
13. Fang F, Pain CC, Piggott MD, Gorman GJ, Copeland GM, de Oliveira CRE, Goddard AJH, Gejadze I. Adjoint data assimilation into a 3D unstructured mesh coastal finite element model. In *Proceedings of the 8th International Conference on Estuarine and Coastal Modeling*, Monterey, CA, 3–5 November 2003, Spaulding ML (ed.), ASCE, 2004; 308–324.
14. Piggott MD, Pain CC, Gorman GJ, Power PW, Goddard AJH. *h*, *r*, and *hr* adaptivity with applications in numerical ocean modelling. *Ocean Modelling*, 2004, in press.
15. Bishop CM. *Neural Networks for Pattern Recognition*. Oxford University Press: Oxford, 1995.
16. Gresho PM, Sani R. *Incompressible Flow and the Finite Element Method*. Wiley: New York, 1998.
17. Hughes TJR, Mallet M. A new finite element formulation for computational fluid dynamics: IV. A discontinuity-capturing operator for multidimensional advective–diffusion systems. *Computer Methods in Applied Mechanics and Engineering* 1986; **58**:329–336.
18. Pain CC, Piggott MD, Goddard AJH, Fang F, Gorman GJ, Marshall DP, Eaton MD, Power PW, de Oliveira CRE. Three-dimensional unstructured mesh ocean modelling. *Ocean Modelling*, 2004, in press.
19. Alekseev AK, Navon IM. On estimation of temperature uncertainty using the second order adjoint problem. *International Journal of Computational Fluid Dynamics* 2002; **16**(2):113–117.
20. Moore AM. Data assimilation in a quasi-geostrophic open-ocean model of the Gulf Stream region using the adjoint method. *Journal of Physical Oceanography* 1991; **21**(3):398–427.

